18èmes Journées Internationales de Thermique (JITH 2017)
Monastir (Tunisie), 25 - 27 Octobre 2017

Emissions characterization in laminar flameless combustion of a hydrogenated biogas

Abdelbaki Mameri[1], Fouzi Tabet[2] and Ammar Hadef[1]

1. Faculté des sciences et sciences appliquées, Département de Génie Mécanique, Université Larbi Ben Mhidi, Oum El Bouaghi, BP 358, 04000, Algeria.
2. DBFZ (Deutsches Biomasseforschungszentrum gemeinnützige GmbH), Torgauer Straße 116 D-04347 Leipzig, Germany.

hadef_am@yahoo.fr, tabethelal@yahoo.fr
mameriabdelbaki@yahoo.fr

Abstract

In this study, the influence of several operating conditions of composition and ambient pressure on flameless (MILD) combustion of biogas are elucidated. Combustion structure and NO emissions are considered with particular attention on chemical effect of CO_2 in the oxidizer. The biogas flameless combustion is modeled by a counter flow diffusion configuration and the GRI Mech-3.0 mechanism that involves 53 species and 325 reactions is adopted for the oxidation chemistry.

It has been noticed that combustion properties are very sensitive to biogas composition and pressure. H_2 increment in the fuel and O_2 augmentation in the oxidizer stream increase combustion temperature, major (CO) and minor (NO and OH) species. Added CO_2 to the oxidizer can contribute in chemical reaction due to thermal dissociation; whereas it plays the role of pure diluent if excessively supplied. The ambient pressure rise induces a non-monotonic variation of maximum temperature and CO mole fraction. At high pressure, recombination reactions coupled with chain carrier radicals reduction, diminishes NO mass fraction.

Keywords

Biogas combustion, flameless combustion, thermal and chemical effects of CO_2 in the oxidizer, pressure effect.

1. Introduction

One of the best solutions for the reduction of environmental problems caused by combustion is the MILD (moderate or intense low-oxygen dilution) combustion regime. In this regime, minimum and maximum temperatures are controlled. In order to identify MILD combustion domain, M. de Joannon et al. [1] studied the influence of fuel percentage and pressure on high temperature oxidizer combustion. The authors used an opposed jet diffusion methane combustion configuration; they varied the fuel mass fraction from 0.05 to 1, pressure took the values 1 and 10 bars and oxidizer injection temperature was 1400K. Results showed a significant spatial change in distribution of heat release associated to oxidant temperature higher than auto-ignition one. The domain where the auto ignition can develop inside constrain of the residence time of the fuel in the system is identified as "MILD-HDDI (Hot-Diluted-Diffusion-Ignition)" combustion region. A combustion diagram is obtained for each pressure and MILD-HDDI limits were clearly identified. Since biogas is a naturally diluted fuel, all its drawbacks can be vanished if it is used in MILD combustion regime. S. E. Hosseini et al have numerically investigated the biogas flameless combustion [2]. Properties of flameless combustion are compared to conventional mode in a three-dimensional computational fluid dynamic study. A two steps chemical kinetics is used with eddy dissipation model for the turbulent combustion and k-ε model for turbulence. It has been found that biogas is not suitable to heat up the furnace due to its low calorific value (LCV) and it is necessary to utilize a high calorific value fuel to preheat the furnace. The authors found that when preheating oxidizer in conventional combustion, fuel consumption decreases however, NOx formation increases drastically. In flameless combustion, NOx formation reduces due to elimination of hot spots and low level of oxygen. Better radiation heat transmission and higher heat capacity are observed for very high concentration of CO_2 species in biogas flameless products. In MILD regime, the oxidizer can be diluted by CO_2 or H_2O, Y. Liu et al. [3] compared this behavior in biogas opposed jet combustion. A biogas composed by volumes of 60% CO_2 and 40%CH_4 is considered, the oxidizer (diluted by CO_2 and then H_2O) is preheated with various

temperature. It has been found that biogas MILD oxy-fuel combustion establishment is easy under H_2O moderation operation, but it is safe to sustain under CO_2 moderation operation. Also, the performance of biogas MILD oxy-fuel combustion under CO_2 moderation operation is always better than its counterpart H_2O. In the same context, P. Sabina et al. [4] considered numerically the effect of diluents on biogas MILD combustion in premixed configuration. The biogas is diluted by CO_2 or H_2O then mixed and preheated up to 1400 K in a tubular flow reactor. The authors showed that the ignition delay times are compatible with the characteristic times required in real facilities. Due to presence of C_2 species, under the same conditions, the ignition delay times are lower than those of methane. The kinetic models used are not able to properly predict auto-ignition delay data, especially when CO_2 or H_2O dilute biogas mixture. MILD combustion of hydrogen blended biogas seems to be the good way of using renewable energy with optimal combustion technology. Few works considered this issue, S. Chen et al. [5] explored a counter flow diffusion flame of hydrogen-enriched biogas under MILD condition. The lattice Boltzmann method (LBM) was used to show the effects of preheating temperature, oxidizer composition and the hydrogen concentration in the fuel mixtures on the reaction structure of biogas under MILD combustion condition. The authors found that MILD combustion is sustained for extremely low-oxygen concentration in the oxidizer flow. Also, MILD combustion of biogas from landfills is better sustained with lower oxygen concentration in the oxidizer flow than higher one. It can be deduced that the use of biogas under the MILD combustion operation up to commercial-scale is possible and its application will significantly reduce the high costs induced by the currently utilizing way.

Although the above survey manifests substantial efforts that have been devoted to flameless combustion, a comprehensive understanding of these combustion structures over a wide range of operating conditions as well as CO_2 chemical effect has not been yet consummated.

The aim of the present study is to investigate biogas diffusion flame structure and emissions in counter-flow configuration over a wide range of operating conditions (hydrogen enrichment, oxidizer dilution and ambient pressure variation) in flameless regime. A special emphasis is put on chemical effect of CO_2 in the oxidizer.

The paper is organized in four sections. Following a brief explanation of the modeling approach, a general description of the simulation details is introduced. The numerical simulation results are then presented with a discussion. The last section summarizes the findings of the present study.

1.1. Formulation of the problem

An axisymmetric geometry, composed by two opposing jets streams configuration, was adopted to analyze the steady unidimensional diffusive reaction zone structure. The Fig. 1 presents the flow geometry, the fuel stream conditions refer to a biogas doped with hydrogen whereas the oxidizer stream one refers to preheated and diluted air by CO_2. The injection velocity is the same for both streams and the distance between injectors is D=2cm.

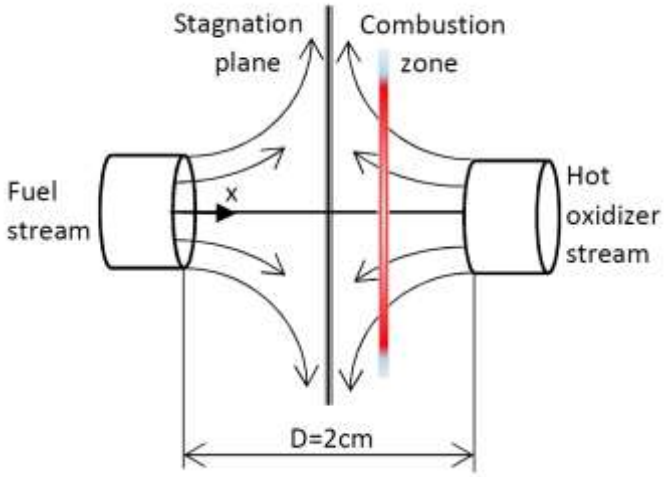

Fig. 1.: Axisymmetric opposed jet flow configuration

1.1.1. Equations of the reacting flow:

Reacting flow equations consisted of the steady state conservation equation in cylindrical coordinates:

$$\frac{\partial \rho u}{\partial x} + \frac{1}{r}\frac{\partial (\rho v r)}{\partial r} = 0 \qquad (1)$$

where ρ, u and v are the density, axial and radial velocity components respectively; r and x represent the radial and axial direction.

The Von Karman hypothesis, which recognized that *v/r* and other variables should be functions of *x* only, simplifies the perpendicular momentum equation (x direction in the Fig. 1) to:

$$H(x) - 2\frac{d}{dx}\left(\frac{F(x)G(x)}{\rho}\right) + \frac{nG^2(x)}{\rho} + \frac{d}{dx}\left[\mu\frac{d}{dx}\left(\frac{G(x)}{\rho}\right)\right] = 0 \qquad (2)$$

where the quantities $G(x) = -\rho v/r$ and $F(x) = \rho u/2$ are only function of x. The continuity equation then reduces to $G(x) = dF(x)/dx$ with ρ and u depending only of x. Therefore, from species and energy equations, Y_k and T should also depend only on x. Species and energy conservation equation are:

$$\rho u\frac{dY_k}{dx} + \frac{d}{dx}(\rho Y_k V_k) - \dot{\omega}_k W_k = 0 \qquad (3)$$

$$\rho u\frac{dT}{dx} - \frac{1}{Cp}\frac{d}{dx}\left(\lambda\frac{dT}{dx}\right) + \frac{\rho}{Cp}\sum_k Cp_k Y_k V_k\frac{dT}{dx} + \frac{1}{Cp}\sum_k h_k\dot{\omega}_k + \frac{1}{C_p}\left[4\sigma p\sum_j X_j a_i(T^4 - T_f^4)\right] = 0 \qquad (4)$$

The ideal gas state equation writes:

$$P = \rho R_u T\sum_k\frac{Y_k}{W_k} \qquad (5)$$

where the diffusion velocities in eq. (4) are given by either the multicomponent formulation:

$$V_k = \frac{1}{X_K\bar{W}}\sum_{j=1}^{k} W_j D_{k,j}\frac{dX_j}{dx} - \frac{D_k^T}{\rho k_k}\frac{1}{T}\frac{dT}{dx} \qquad (6)$$

With D_k, j and D_k^T are the multicomponent and thermal diffusion coefficients, respectively. The last term in Eq. (4) is the radiation heat loss resulting from the optically thin model. In this term, σ , P, X_j and T_f are the Stefan-Boltzmann constant, pressure, j*th* species mole fraction and the far-field temperature, respectively. The a_i are the polynomial coefficients for the Planck mean absorption coefficients. The gaseous species that participate in radiation are CH_4, CO, CO_2, and H_2O.

1.1.2. Injection conditions

The injection conditions for the fuel and oxidizer streams at the nozzles are summarized in the table 1.

Table 1: Injection values for different parameters

	Fuel stream	Oxidizer stream
Velocity	$v_F = \left[\frac{aD}{2} - 1\right]\sqrt{\frac{\rho_O}{\rho_F}}$ (m/s)	$v_O = v_F$ (m/s)
Temperature	300 (K)	1200 (K)
X_{CH4}	0.4	0
X_{CO2}	0.6	0.11 to 0.19
X_{O2}	0	0.02 to 0.10
X_{H2}	0.1 to 0.2	0

The set of differential equations and boundary conditions form a boundary value problem which is resolved by CHEMKIN program.

1.2. Simulation details

The resolution of the differential equations is achieved assuming multicomponent diffusion transport for all species participating in the chemical mechanism. The radiative heat loss flux from the reaction zone is modeled by the optically thin model. The kinetics of combustion is described by the GRI 3.0 mechanism [6], which is composed of 325 reactions involving 53 species. A low-grade biogas is considered, BG40 (40% methane and 60% carbon dioxide), with several doping values of H_2 in the fuel and O_2 molar fraction in the oxidizer. Computations are performed for the following conditions: ambient pressure ranges from 1 to 10 atm, H_2 molar ratio from 0 to 20%, O_2 molar fraction from 2% to 10% and strain rate a = 200 s^{-1}.

The main species composing biogas are CO_2 and CH_4, the combustion chemistry of these species is well described by the GRI 3.0. The accuracy of this mechanism was intensively evaluated in previous studies dedicated to hydrocarbons in MILD combustion regime employing experimental data and prediction. For example, in a parallel jet burner system operating in MILD combustion, G.G. Szego et al. [7] have used the GRI-3.0 mechanism to study the operational characteristics of the burner. Results shows good concordance with experience when using this mechanism. In a recent paper, G. Sorrentino et al. [8] used GRI 3.0 mechanism in the investigation of the ignition

and annihilation of methane/nitrogen/oxygen mixture under MILD combustion. In another study [9] the authors used GRI-3.0 mechanism and verified across various conditions that kinetic mechanism is able to predict the general behavior of systems working in MILD conditions [10].

2. Results and discussions

2.1. Hydrogen and oxygen contents effect on flame structure

To investigate the flame characteristics response to the hydrogen addition to the fuel and the oxygen content of the oxidizer, the low-quality biogas BG40 (40% CH_4 and 60% CO_2) is doped by a volume of hydrogen varying from 0 to 20% and the oxidizer is enriched by a volume of oxygen from 2 to 10%, here, it should be mentioned that doping or addition operations consist of the replacement of a volume of the fuel or oxidizer by the same volume of hydrogen or oxygen respectively. In this section, ambient pressure is 1atm and the strain rate is kept constant and equal to 200 s^{-1}, this makes the velocity variable with composition but it is the same for both fuel and oxidizer jets. First, results of adiabatic flame temperature are shown followed by flame structure and NO emission.

Fig. 2 depicts the biogas adiabatic flame temperature variation in function of oxygen molar fraction, which varies from 2 to 10% in the oxidizer stream, and the hydrogen enrichment, which increases from 0 to 20% in the fuel stream. Adiabatic flame temperature, which is obtained from thermodynamic equilibrium calculation [11], increases linearly with O_2 addition to the oxidizer. For a fixed oxygen molar fraction in the oxidizer and increased hydrogen in the fuel, adiabatic flame temperature grows very slow. Indeed, for O_2 = 2% in the oxidizer and H_2 = 0% in the fuel, the adiabatic flame temperature is 1400 K, it increases only by 6K while H_2 reaches 20%. Whereas, for O_2=10% in the oxidizer and H_2 = 0% in the fuel, the adiabatic flame temperature is 2017 K and rises by 27K for H_2 = 20%.

For a fixed hydrogen molar fraction in the fuel and increased oxygen in the oxidizer, adiabatic flame temperature grows sharply. For 0% of H_2 in the biogas and O_2 = 2% in the oxidizer, the adiabatic flame temperature is 1400 K, it increases by 647K while the O_2 volume reaches 10%. For 20% of hydrogen addition to the fuel and 2% of oxygen in the oxidizer, the adiabatic flame temperature is 1406 K and rises by 638 K while the volume of oxygen in the oxidizer is 10%.

At low oxygen concentration in the oxidizer, which is relevant to MILD combustion (from 2% to 5%) [12], adiabatic flame temperature is more sensitive to oxygen in the oxidizer than hydrogen in the fuel.

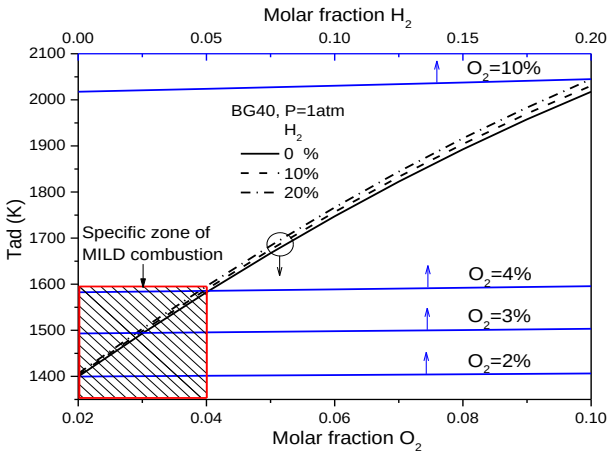

Figure 2: Effects of hydrogen addition to the fuel And oxygen to the oxidizer on the adiabatic flame temperature.

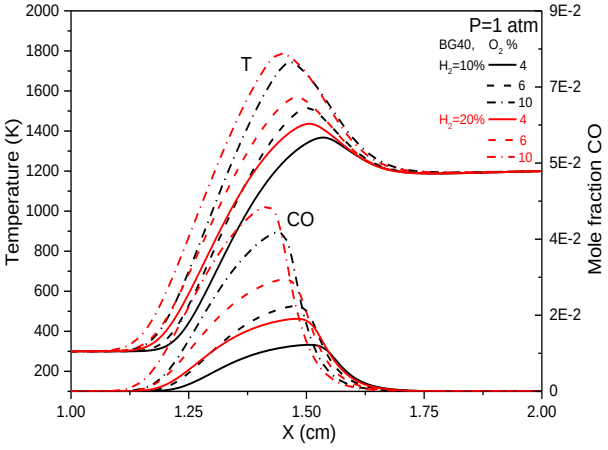

Figure 3: Variation of temperature and CO mole fraction in function of the flame cross section distance and hydrogen addition to the fuel.

The Fig. 3. depicts combustion temperature and CO mole fraction profiles of the BG40 biogas doped by 10% and 20% of hydrogen with an oxidizer enriched by a volume of 4% to 10% of oxygen. Here, it should be mentioned that temperature increases with hydrogen addition because hydrogen is more diffusive and has an important LHV compared to methane, enrichment by hydrogen makes the mixture more reactive [13]. Reducing oxygen in the oxidizer stream to meet MILD regime, reduces combustion temperature significantly. For 4% oxygen and 10% hydrogen, the maximum temperature is 1367K, it increases by 69K when hydrogen increases to 20%. For 10% oxygen and 10% hydrogen, the maximum temperature is 1744K, it increases by 44K when hydrogen increases to 20%. It can be seen from temperature profiles in Fig. 3. that MILD regime prevails nearly until 6% of oxygen, after that the temperature increases rapidly and the MILD regime breaks down. Temperature profiles are all shifted to the fuel side in response of hydrogen or oxygen increases. Also from Fig. 3., it can be noticed that CO mole fraction is increased by hydrogen addition to the fuel and oxygen increment in the oxidizer with a shift of CO peak value to

the fuel side. In MILD combustion regime, characterized by a small amount of oxygen (2 to 5%) in the oxidizer, the CO mole fraction is reduced significantly.

From Fig. 4., H_2 augmentation in the fuel and O_2 increasing in the oxidizer increase the mole fraction of OH radical. The same behavior has been mentioned in previous studies [14]. OH is produced in a narrow region which is shifted towards the fuel side with H_2 and O_2 additions. For all cases, the width of the OH produced zone does not exceed 0.37 cm in X space.

Also in Fig. 4, the NO mole fraction decrease with O_2 reduction in the oxidizer stream and increases with hydrogen addition to the fuel. NO is maximal at temperature peaks; the low temperature levels of the MILD combustion regime inhibits NO formation. For MILD regime conditions, while oxygen volume is 4% and hydrogen one is 10%, the maximum NO mole fraction is 0.58 ppm, it increases to 2.6 ppm when hydrogen increases to 20%. When MILD regime breaks, for 10% oxygen and 10% hydrogen, the maximum NO mole fraction is 28 ppm, it increases to 38 ppm when hydrogen increases to 20%.

2.2. Pressure effects on maximum properties

The figures 5 to 8 present the effects of ambient pressure, hydrogen addition to the fuel and oxygen addition to the oxidizer on the maximum properties of the combustion. The values reported for hydrogen are H_2=10% and 20% those for oxygen are 4%, 6% and 10% and finally ambient pressure ranged from P=1atm to 10 atm.

In Fig. 5, the maximum temperature is presented. It is noticed that for the small amounts of hydrogen in the fuel (0 to 5%) and oxygen in the oxidizer (0 to 7%) no combustion occurs for all values of ambient pressure. When hydrogen or oxygen are above the mentioned limits, the mixture reacts nearly for all ambient pressures. It can be seen from Fig. 5. that for the case of 4% oxygen and 10% hydrogen, the temperature decreases when pressure increases which is not conform to the conventional combustion regime. For the other cases included in the MILD regime, 4% to 6% oxygen with 10% to 20% hydrogen, the temperature exhibits a non-monotonic behavior with a maximum value when pressure rises. For the case of 4% oxygen and 20% of hydrogen, the maximum temperature is 1447K located at P=2.5 atm while for 6% of oxygen and 10% of hydrogen the maximum temperature is 1530 K located at P=2.5 atm. In the case of 6% oxygen and 20% hydrogen the maximum temperature is 1617K located at P=8 atm. When the MILD regime breaks (the cases of 8% oxygen), the temperature shows an increasing slope in function of pressure, which is the case of the conventional combustion regime.

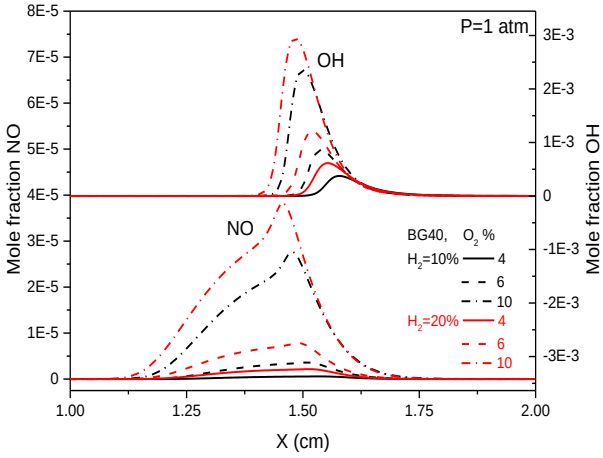

Figure 4: Variation of OH and NO mole fractions in function of the flame cross section distance and hydrogen addition to the fuel.

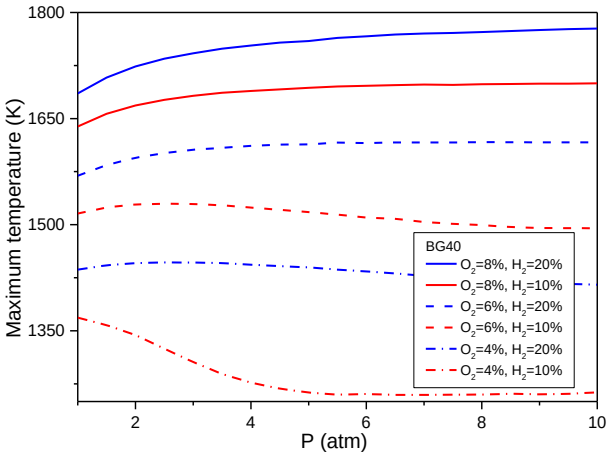

Figure 5: Variation of maximum temperature in function of the pressure, oxygen and hydrogen addition.

In the fig. 6. it can be noticed that the maximum CO mole fraction varies inversely to maximum temperature. Indeed, in the MILD combustion regime, the maximum CO mole fraction shows a non-monotonic variation with a minimum value when pressure augments. Whereas in the conventional regime it is fully decreasing with pressure increase.

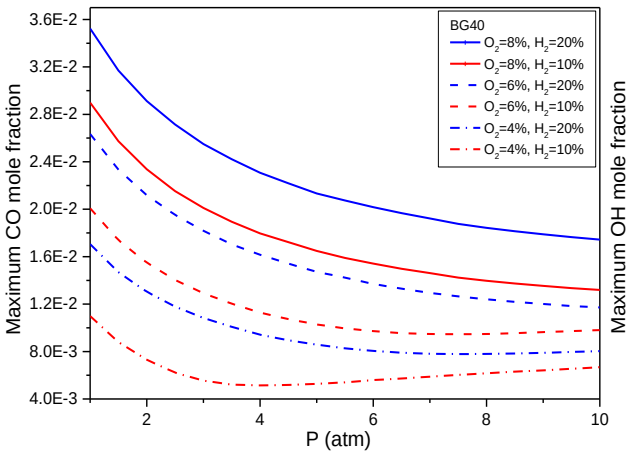

Figure 6: Variation of maximum CO mole fraction in function of the pressure, oxygen and hydrogen addition.

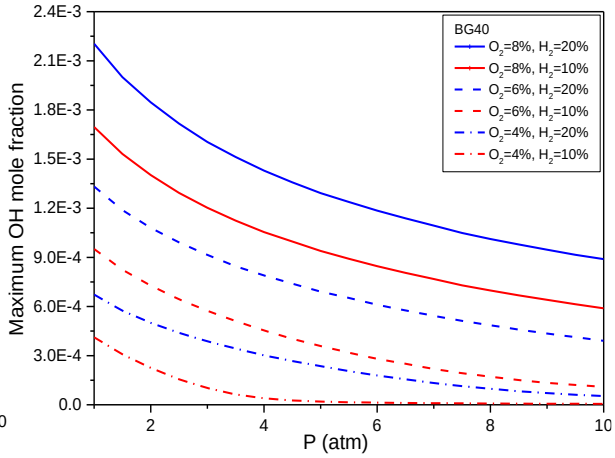

Figure 7: Variation of maximum OH mole fraction in function of the pressure, oxygen and hydrogen addition.

The fig. 7. shows that maximum OH radical mole fraction decreases in all cases with pressure. It can also be noticed that the decrease is more pronounced in the MILD regime. The maximum NO mole fraction is presented by the Fig. 8, which shows a monotonic decrease in function of pressure for both MILD and conventional combustion regimes. It is important the notice that maximum NO mole fraction is drastically reduced in the MILD combustion regime.

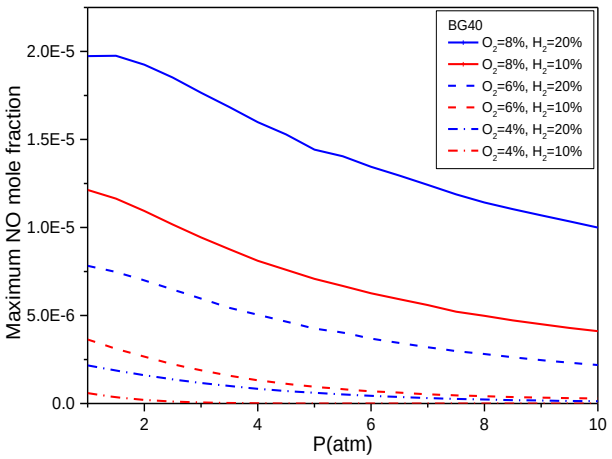

Fig. 8.: Variation of maximum NO mole fraction in function of the pressure, oxygen and hydrogen addition.

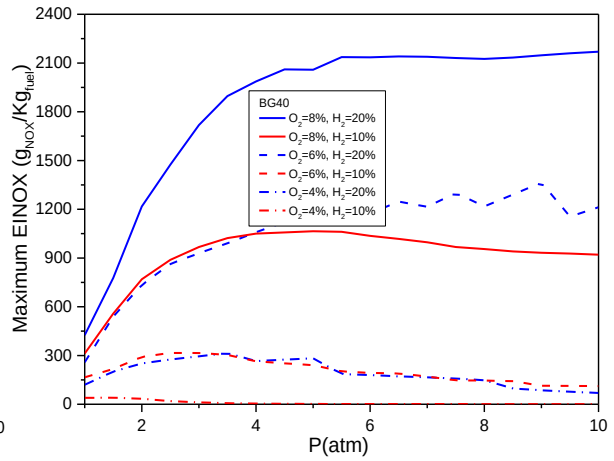

Figure 9: Variation of the maximum EINOx in function of the pressure, oxygen and hydrogen addition.

2.3. The NOx emission index

To characterize NOx emission, the global emission index, EINOX, is introduced [15]:

$$\mathrm{EINOx} = \frac{\int_0^1 W_{\mathrm{NOx}}\dot{w}_{\mathrm{NOx}}dz}{\int_0^1 W_{\mathrm{fuel}}\dot{w}_{\mathrm{fuel}}dz} = \frac{\int_0^1 W_{\mathrm{NOx}}\dot{w}_{\mathrm{NOx}}dz}{\int_0^1 \left(W_{\mathrm{H_2}}\dot{w}_{\mathrm{H_2}} + W_{\mathrm{CH_4}}\dot{w}_{\mathrm{CH_4}} + W_{\mathrm{CO_2}}\dot{w}_{\mathrm{CO_2}}\right)dz} \qquad (7)$$

where W_i and $\dot{w}_i$ are molecular weights and molar production rates of i*th* species, ($i = \mathrm{NOx}, \mathrm{H_2}, \mathrm{CH_4}$ and $\mathrm{CO_2}$) respectively.

Fig. 9 depicts the variation of EINOx emissions index for BG40 in function of hydrogen volume in the fuel, oxygen volume in the oxidizer for different ambient pressure. In the case of MILD combustion regime, the EINOx shows a non-monotonic trend with maximum values as function of ambient pressure. After EINO has reached its maximum values, it begins deceasing monotonically to its minimum ones at the end of the ambient pressure range. It is, also, seen that EINOx is increased by H_2 and O_2 increments in the fuel and oxidizer respectively. EINOx is lowered significantly in the MILD combustion regime compared to conventional regime. Hydrogen blending increases EINOx for both regimes, however EINOx augmentation is significant in conventional regime. In addition,

it can be observed that BG40-20%H_2-4%O_2 and BG40-10%H_2-6%O_2 have nearly the same EINOx level especially for elevated ambient pressure where low NO emissions are obtained for all hydrogen volumes considered.

2.4. Chemical effect of the CO_2 contained in the oxidizer

Fig. 10 illustrates the chemical effect of the CO_2 present in the oxidizer on the maximum values of temperature CO, OH and NO for pressure ranging from 1 to 10 atm. The study is conducted for BG40 doped with 10% and 20% of hydrogen. CO_2 mole fraction in the oxidizer is 0.17. The artificial inert species X_CO_2 method is adopted in order to highlight the CO_2 chemical effect. This species has the same transport, radiation and thermochemical properties of CO_2. Therefore, the difference between calculated combustion properties with the artificial species X_CO_2 and CO_2 is due to the chemical effects of added CO_2.

Fig. 10 shows that the CO_2 chemical effect reduces the peak value of the temperature especially in the case of 10% hydrogen enrichment. For 10% hydrogen in the fuel, the chemical effects exhibits a non-monotonic variation with pressure, it reaches its maximum for P=5 atm with $\Delta T=T_{max,X\_CO2}-T_{max,CO2}$ = 195K. For 20% hydrogen the chemical effects increases linearly in function of pressure for P = 1atm the difference temperatures caused by CO_2 chemical effects is $\Delta T=T_{max,X\_CO2}-T_{max,CO2}$ =80 K it grows to $\Delta T=T_{max,X\_CO2}-T_{max,CO2}$ =130 K for P = 10 atm.

From Fig. 11, it can be seen that CO_2 chemical effect increases the maximum value of CO mole fraction. This increase is more important in the case of 20% hydrogen. The chemical effect of CO_2 on CO shows a non-monotonic variation with pressure augmentation for both cases of hydrogen addition to the fuel (10% and 20%). For 10% and 20 % hydrogen, the maximum chemical effect of CO_2 on CO is reached at P= 3.5 atm and P= 6 atm respectively.

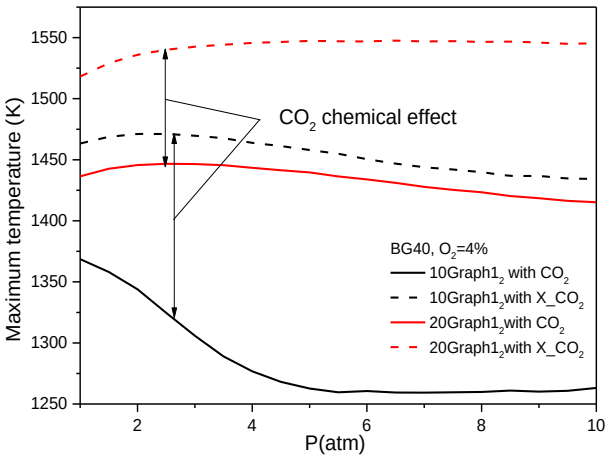

Figure 10: The chemical effect of CO_2 on maximum temperature.

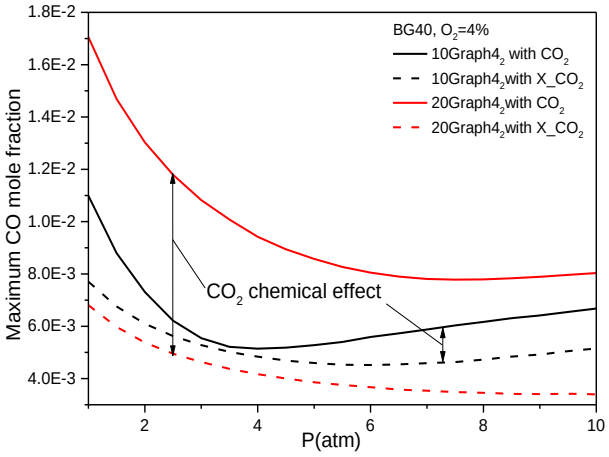

Figure 11: The chemical effect of CO_2 on maximum CO mole fraction.

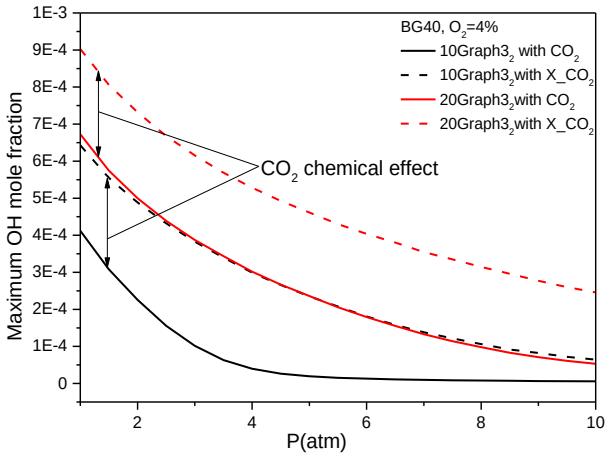

Figure 12: The chemical effect of CO_2 on maximum OH mole fraction.

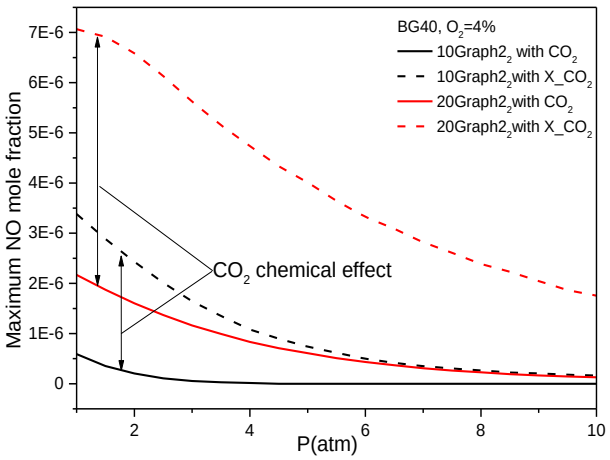

Figure 13: The chemical effect of CO_2 on maximum NO mole fraction.

Fig. 12 presents the CO_2 chemical effect on the radical OH; maximum OH mole fraction is reduced by the chemical effect of CO_2 present in the oxidizer. For the case of 10% of hydrogen in the fuel, the chemical effect

exhibits a non-monotonic variation with pressure, it reaches its maximum for P=3 atm. For 20% hydrogen the chemical effects decreases linearly in function of pressure to reach its minimum value at P= 10atm.

Fig. 13 presents the CO_2 chemical effect on the NO mole fraction; maximum NO mole fraction is reduced by the chemical effect of CO_2 present in the oxidizer. Chemical is more pronounced for the case of 20% hydrogen added to the fuel. For both cases of 10% and 20% of hydrogen in the fuel, the chemical effect exhibits a decreasing trend with pressure it reaches its minimum values at P= 10atm.

Conclusion:

Flameless (MILD) combustion of biogas was studied numerically and emissions were characterized. The H_2 volume in the fuel was varied from 0% to 20%, the O_2 volume in the oxidizer stream ranged from 2% to 10% (where the oxygen of the air is replaced by CO_2 from 11 to 19%) and ambient pressure increased from 1 to 10 atm. The chemical effects of CO_2 on combustion temperature and emissions was also investigated. The following conclusions can be drawn:

Hydrogen increase in the fuel or oxygen augmentation in the oxidizer increases the MILD combustion temperature, species concentrations, NO emissions and EINOX. At low hydrogen (0% to 5%) and oxygen (2% to 6%) concentrations, combustion didn't occur for all pressure values until oxygen is increased in the oxidizer. An increase of oxygen volume in the oxidizer above 5% breaks down the MILD combustion regime for the hydrogen volume above 10%.

Pressure increase, in the MILD combustion regime, reduces all presented species except CO and temperature which show a non-monotonic behavior with a minimum and maximum value respectively. When pressure increases in MILD combustion, the NO and EINOX are reduced drastically.

Except CO species, the CO_2 increase in the oxidizer reduces all presented species and temperature by chemical effect. For temperature and CO species, the CO_2 chemical effect in function of pressure shows different trends depending on hydrogen concentration in the fuel and oxygen volume in the oxidizer.

Nomenclature

a: strain rate s^{-1}
a_i: mean absorption coefficients of Plank for species i
C_p: specific heat at constant pressure, J kg^{-1} K^{-1}
D_Z: diffusion coefficient m^2s^{-1}
H_i: Enthalpy of species i, J kg^{-1}
Le: Lewis number
LHV: Lower Heating Value
P: Operating pressure, atm
N_i : Number of moles of species i, moles
s: Stoichiometric mass ratio of oxygen to fuel
T: temperature, K
X_i: Species i, mole fraction
Y_i: Species i, mass fraction
Y_{FF}: Feed stream mass fraction of the fuel
Y_{OO}: Feed stream mass fraction of the oxygen
Z: Mixture fraction

Greek letters:
λ: Thermal conductivity, W $m^{-1}K^{-1}$
ρ: Density, kg m^{-3}
σ: Steffan-Boltzmann constant, 5.669 x 10^{-8} W m^{-2} K^{-4}
χ: Scalar dissipation rate, s^{-1}

Subscripts:
f: far field value
hinj: hot injection
comb: combustion
i: species i
st: stoichiometric
∞: Oxidizer side

References

[1] Mara de J, Sabia P, Sorrentino G, Cavaliere A. Numerical study of mild combustion in hot diluted diffusion ignition (HDDI) regime. Proceedings of the Combustion Institute 32 (2009) 3147–3154.

[2] Hosseini S E, Ghobad B, Mazlan A W. Numerical investigation of biogas flameless combustion. Energy Conversion and Management, 2014;81 :41-50

[3] Yaming L, Sheng C, Bo Y, Kai L, Chuguang Z. First and second thermodynamic-law comparison of biogas MILD oxy-fuel combustion moderated by CO_2 or H_2O. Energy Conversion and Management, 2015;106 :625-634.

[4] Pino S, Marco L L, Giancarlo S, Paola G, Raffaele R, Mariarosaria J. H_2O and CO_2 Dilution in MILD Combustion of Simple Hydrocarbons. Flow, Turbulence and Combustion, 2016;96(2): 433-448.

[5] Sheng C, Chuguang Z. Counterflow diffusion flame of hydrogen-enriched biogas under MILD oxy-fuel condition. International Journal of Hydrogen Energy, 2011;36(23) :15403-19413.

[6] Gregory P. Smith, David M. Golden, Michael Frenklach, Nigel W. Moriarty, Boris Eiteneer, Mikhail Goldenberg, C. Thomas Bowman, Ronald K. Hanson, Soonho Song, William C. Gardiner, Jr., Vitali V. Lissianski, and Zhiwei Qin http://www.me.berkeley.edu/gri_mech/

[7] Szego G G, Dally BB, Nathan G J. Operational characteristics of a parallel jet MILD combustion burner system. Combustion and Flame, 2009;156: 429–438.

[8] Giancarlo S, Mariarosaria J, Pino S, Raffaele R, Cavaliere A. Numerical investigation of the ignition and annihilation of $CH_4/N_2/O_2$ mixtures under MILD operative conditions with detailed chemistry. Combustion Theory and Modelling, http://dx.doi.org/10.1080/13647830.2016.1220624

[9] Mara de J, Sorrentino G, Cavaliere A. MILD combustion in diffusion-controlled regimes of Hot Diluted Fuel. Combustion and Flame, 2012;159(5): 1832-1839.

[10] Mara J, Pino S, Giancarlo S, Cavaliere A. Proc. Combust. Inst. 2008;2: 3147–3154.

[11] El Bakali A, Pillier L, Desgroux P, Lefort B, Gasnot L, Pauwels JF, et al. NO prediction in natural gas flames using GDF-Kin®3.0 mechanism NCN and HCN contribution to prompt-NO formation. Fuel 2006;85(7-8):896-909

[12] Mara J, Langella G, Beretta F, Cavaliere A, Noviello C. Reactor characteristics related to moderate or intense low oxygen dilution for clean/cleaning combustion plants. Clean Air. Int J Energy Clean Environ 2003;4(1):1–20.

[13] Mameri A. Etude numérique de la combustion turbulente du prémélange pauvre méthane/air enrichi à l'hydrogène. Ph.D Thesis, Université d'Orléans, France, 2009.

[14] Mameri A, Tabet F (2016) Numerical investigation of counter-flow diffusion flame of biogas–hydrogen blends: Effects of biogas composition, hydrogen enrichment and scalar dissipation rate on flame structure and emissions. International Journal of Hydrogen Energy 41: 2011-2022

[15] Nishioka M, Nakagawa S, Ishikawa Y, Takeno T. NO emission characteristics of methane-air double flame. Combustion and Flame 1994; 98(1-2):27-138.